Received: 8 September 2023 | Revised: 10 July 2024 | Accepted: 19 July 2024

DOI: 10.1111/csp2.13211

SCIENTIFIC IMPACT PAPER

Conservation Science and Practice
A Journal of the Society for Conservation Biology
Open Access

WILEY

Landscape changes of alpine grasslands in the Zhari Namco basin of the central-southern Qiangtang plateau, 2001–2021

Lu Chen[1] | **Wei Zhang**[2] | **Wenjie Li**[3] | **Huixin Zhang**[1] | **Shijia Luo**[1] | **Qinghong Ran**[1] | **Jianxiong Qin**[4,5]

[1]Sichuan Province Key Laboratory of Philosophy and Social Sciences for Rural Land Use Monitoring and Assessing, Chengdu Normal University, Chengdu, China

[2]Faculty of Geography and Resources Science, Sichuan Normal University, Chengdu, China

[3]Beijing Minhoo Technology Co., Ltd, Beijing, China

[4]College of Historical Culture and Tourism, Southwest Minzu University, Chengdu, China

[5]College of Physics and Engineering, Chengdu Normal University, Chengdu, China

Correspondence
Wei Zhang, 5# Jing'an Road, Jinjiang District, Chengdu City, Sichuan Province, China.
Email: 185518853@qq.com

Funding information
The Key Project of Sichuan Province Key Laboratory of Philosophy and Social Sciences for Rural Land Use Monitoring and Assessing, Grant/Award Number: NDZDS202402; The Major Project of Sichuan Primary and Secondary School Teacher Professional Development Research Center, Grant/Award Number: PDTR2022-03; Chengdu Normal University high-level research project, Grant/Award Number: CS22XMPY0115; Chengdu Normal University talent introduction project, Grant/Award Number: YJRC2016-6

Abstract

The alpine grasslands of the Qiangtang Plateau face significant ecological risks due to extensive human activities, particularly in areas along lakeshores and riverbanks, where overgrazing has caused severe degradation and salinization of the grasslands. Conducting fieldwork in such environments presents significant challenges for long-term community-scale landscape ecological research. In this study, the habitat characteristics of dominant plant communities in the alpine basin of Zhari Namco were quantified from three perspectives: topography, hydrology, and fractional vegetation cover. Using Aster GDEM and Landsat imagery, five grassland types were mapped for 2001–2021. Based on the spatial variables of area, shape, and distance, 13 landscape indices were selected to observe spatiotemporal changes. The results revealed several key findings: (1) The patch structure of the zonal vegetation *Stipa purpurea* steppe has undergone a pattern of dispersion-aggregation-dispersion in the past 20 years, yet the core habitat area remains unchanged by more than 52%, indicating fundamental stability in the southern Qiangtang alpine grassland; (2) Using the minimally grazed *Kobresia pygmaea* meadow as a reference, other communities exhibit stability similar to or approaching it, but with significant differences in aggregation level. The gradual expansion of grazing and economic activities has been a driving factor; and (3) Water conservation projects have diversified the use of water resources in river and lakeside habitats. *Stipa purpurea* + *Carex moorcroftii* steppe and *Carex* swamp meadow exhibit optimal carrying capacity, making them the only areas with relatively high sustainability. The study underscores that the current ecological benefits are a

This is an open access article under the terms of the Creative Commons Attribution License, which permits use, distribution and reproduction in any medium, provided the original work is properly cited.
© 2024 The Author(s). *Conservation Science and Practice* published by Wiley Periodicals LLC on behalf of Society for Conservation Biology.

result of effective management. However, without proper management, the region could trend towards landscape fragmentation, becoming the most vulnerable zone in the watershed. Therefore, it is essential to strengthen retrospective analysis of grazing intensity and trend analysis of habitat changes to provide a scientific basis for local economic development and grazing management.

KEYWORDS

alpine grasslands, central-southern Qiangtang plateau, endemic community types, habitat type, landscape change, Zhari Namco basin

1 | INTRODUCTION

The alpine grasslands are mainly distributed in high latitude and altitude regions globally (Scholtz & Twidwell, 2022), garnering significant attention in ecosystem functionality, climate change responses, and grassland utilization management (Dong et al., 2020; Filippa et al., 2022; Rossi et al., 2020). Vegetation in alpine grasslands is sensitive to both natural and human impacts. Changes in plant communities offer crucial evidence at the landscape scale (Zimmermann & Kienast, 1999). Identifying and accurately classifying community types, as well as their spatial distribution, are fundamental for ecological research (Kong et al., 2019). Today, automated extraction technologies in remote sensing data precisely delineate land covers with significant heterogeneity (Liu et al., 2021; Pottier et al., 2014; Yang et al., 2022). However, classifying grasslands based on plant communities remains challenging when using spectral imagery (Chetan et al., 2018). Some researchers have discerned various plant community types with distinct phenological features by utilizing spectral information from annual plant growth cycles (Lewińska et al., 2020; Weber et al., 2018). Nonetheless, the short growing season and similar vegetation phenological features complicate the delineation of plant communities, posing a significant disadvantage.

The vast Qiangtang Plateau, located in the tectonic lake basins of northern Tibet, serves as the primary distribution area for alpine grasslands in China. With a pastoral heritage spanning thousands of years, the landscape patterns of the Qiangtang Plateau have remained largely unchanged over several decades or even centuries. However, characteristic changes occurring over consecutive years often remain hidden within the processes at certain sub-scales of the overall system. Literature analysis reveals a notable correlation between temporal scale, spatial scale, and plant community type scale. Long-term time series data spanning decades have been collected for the entire plateau (Ma, 2021) or typical regions (Wang & Zheng, 1999), with areas such as the Three Rivers Source and the Ruoergai Plateau (Chen & Lu, 2010; Wang et al., 2022; Wen et al., 2022) continuously attracting research attention. Research typically revolves around wetlands, meadows, and steppes. For unique habitats such as perennial permafrost areas, plateau mining areas, or fenced experimental areas (Qian et al., 2020; Xie et al., 2022; Zhu et al., 2020), researchers have collected shorter time-series data, covering periods of a year or a few years, with a focus on dominant community scales. However, discussions concerning long-term time series accompanied by landscape ecology at the community scale are relatively rare.

The Qiangtang Plateau boasts a series of endorheic lakes, including Namco, Selinco, Tangra Yumco, and Zhari Namco, all situated along the northern foothills of the Nyenchen Tanglha and Gangdise mountains. Alpine grasslands are widely distributed across various lakeside plains, small undulating mountains, and high-elevation terrain, typically at an average altitude of 4000–4600 m, exhibiting characteristics of plateau zonation (Zhang, 1978). Ecologists in the 1990s confirmed that factors such as topography and hydrology govern vegetation distribution patterns at both landscape and community scales (Kikuchi, 1990; Ostendorf & Reynolds, 1998), as well as in the mapping of alpine grassland communities (Zimmermann & Kienast, 1999). Comparing multi-source data for spectral diversity and environmental heterogeneity modeling indicates that plant diversity characteristics at the landscape scale, heavily influenced by habitat type, can also be identified through spectral features (Perrone et al., 2023). Both zonal climatic conditions and non-zonal environmental factors collectively determine the geographical distribution of alpine grassland vegetation types. By quantifying plateau zonal factors and environmental influences, the factors influencing the geographical distribution of alpine grassland vegetation types can be quantified. Consequently, this shift will transform the classification of grassland vegetation types into habitat

type classification, facilitating the establishment of distribution patterns for dominant grassland communities.

Building on this knowledge, topographical factors (altitude, slope, aspect, and relief), hydrological factors (depth of depressions), and fractional vegetation cover (FVC), were selected as indicators for habitat classification in the vicinity of the Zhari Namco basin, a relatively large structural basin situated in the central region of the South Qiangtang Plateau. Distribution maps of grassland plant community types for the years 2001, 2006, 2012, 2016, and 2021 were generated using field surveys, repeated tests, digital elevation models (DEMs), and Landsat imagery. Landscape indices are widely applied in Land Use/Land Cover analysis, facilitating the analysis of landscape patterns and processes across various scales, from local to regional (Wang et al., 2023). This study employs a landscape index approach, coupled with transfer analysis, to evaluate the spatiotemporal dynamics of alpine grassland communities in the study area from 2001 to 2021. The aim is to assess the landscape structure and ecosystem status of these communities while analyzing their relationship with pastoral economy and water infrastructure development.

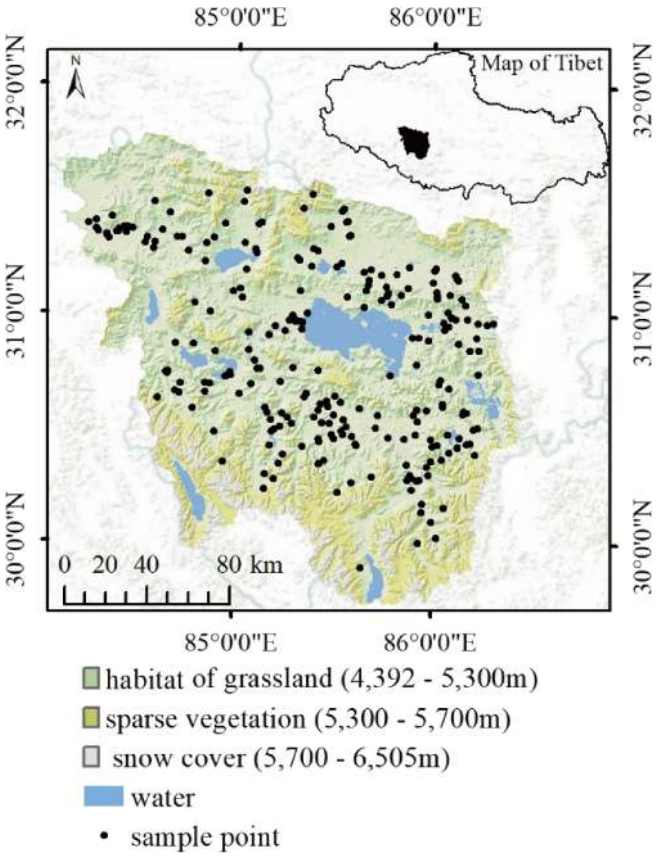


FIGURE 1 Location of Zhari Namco basin in Tibet and the distribution of 250 sample points.

2 | MATERIALS AND METHODS

2.1 | Overview of the study region

The Zhari Namco basin, situated in the hilly, mountainous subregion of South Qiangtang, lies within the coordinates E84°05′38″–86°27′24″ and N29°42′39″–31°48′46″. Encompassing an area of approximately 4.01×10^3 km^2, it ranges in elevation from 4392 to 6505 m, with higher terrain in the south and lower terrain in the north (Figure 1). This area experiences a typical plateau semi-arid continental climate, characterized by an average annual temperature below 0°C, and annual precipitation ranging from 150 to 300 mm, predominantly concentrated between June and September (Tibetan Plateau Comprehensive Scientific Expedition Team, 1984). Extensive literature reviews (Editorial committee of vegetation map of China, 2007; Tibet Autonomous Region Bureaus of Land Administration and Animal Husbandry, 1994; Tibetan Plateau Comprehensive Scientific Expedition Team, 1988) and field surveys have identified five main types of grazing grassland communities in the Zhari Namco basin. Alpine steppes dominated by *Stipa purpurea* (*S. purpurea*) spread extensively below 5200 m in well-drained open areas such as hillocks, alluvial fans, and eroded plateau planation surface, constituting the basal zone of the southern Qiangtang alpine grasslands (Tibetan Plateau Comprehensive Scientific Expedition Team, 1983). Communities dominated by *Stipa purpurea* + *Carex moorcroftii* (*S. purpurea* + *C. moorcroftii*) steppe occupy sunnier and semi-sunny slopes with drier geographic conditions. Alpine meadows dominated by *Kobresia pygmaea* (*K. pygmaea*) thrive between 4800 and 5300 m on the upper slopes of high mountains, boasting relatively moist soil and higher vegetation coverage compared to steppes. Additionally, two intrazonal grassland types, *Carex* spp., (*Carex*) swamp meadow and *Kobresia littledalei* (*K. littledalei*) meadow exist in lakeside plains, waterlogged areas along rivers, low-elevation terraces, and at the outer edges of alluvial fans, all situated at elevations of 4400–5200 m. Due to the high groundwater levels, flat terrain, and excellent hydrothermal conditions, these grasslands exhibit the highest vegetation coverage. However, their geographical distribution is limited, accounting for a small proportion of the study region. While the first three types demonstrate a pattern of altitudinal zonation, the last two types are greatly influenced by topography and hydrology.

Ninety percent of the basin falls under the jurisdiction of Coqen County, with the vast range of mountains and hills in the southeast governed by Ngamring County and the smaller range of wide mountain valleys and

piedmont alluvial fans in the northeast managed by Nyima County. Within this area, the agricultural economy is predominantly pastoral, and the rapid growth in construction and service industries has been ongoing since the beginning of the century. In addition to climatic influences, the main anthropogenic factors affecting changes in these grassland landscapes include grazing-focused grassland utilization and a self-sufficient pastoral economy (Zhang et al., 2020).

2.2 | Data source and processing

The Landsat remote sensing imagery utilized in this study was sourced from the US Geological Survey (USGS, http://glovis.usgs.gov/). Multiple field surveys have revealed that grasslands typically begin to green from late May to early June, transitioning to yellow in the above-ground sections by mid to late September. During the growing season, there is synchronization between water and heat, leading to increased cloud cover, which in turn limits optimal imaging periods. To mitigate this, imagery with cloud cover ≤10% was collected during the grassland growth seasons spanning May 8 to September 27 for the years 2001, 2006, 2012, 2016, and 2021, resulting in four scenes per year and totaling 20 scenes (Table 1). The DEM used was ASTER GDEM V3, obtained from the Geospatial Data Cloud of the Computer Network Information Center, Chinese Academy of Sciences. This dataset, jointly released by NASA and METI on August 5th, 2019, includes an additional 360,000 optical stereo pairs of data. This augmentation was aimed at minimizing gaps in elevation values and correcting numerical anomalies in water bodies. Topographic factors extracted from this dataset exhibit superior quality compared to prior versions. After integrating the DEM into ArcGIS 10.6 software, the delineation of the Zhari Namco basin was performed using its hydrological analysis function. Subsequently, utilizing the ENVI 5.6 software, images from different periods were seamlessly stitched together and cropped in accordance with the DEM of the study region. The data were managed in raster format, with the projection coordinate system set to WGS_1984_UTM_Zone_45N and the spatial resolution set to 30 m.

To identify plant community types, the 1:1000,000 Chinese Vegetation Atlas was utilized, sourcing its data from the Western China Environmental and Ecological Science Data Center of the National Natural Science Foundation of China. For landscape type verification, the 1:250,000 Soil Type Distribution Map of Coqen County

TABLE 1 Information of the Landsat images.

Year	Date	Mission identifier	Cloud cover (%)	Wrs path/row	Level
2021	16.05	Landsat 8	6.63	141/039	L2SP
	23.05	Landsat 8	7.06	142/038	L2SP
	23.05	Landsat 8	6.94	142/039	L2SP
	21.09	Landsat 8	7.89	141/038	L2SP
2016	18.05	Landsat 8	2.86	141/038	L2SP
	18.05	Landsat 8	2.52	141/039	L2SP
	25.05	Landsat 8	4.52	142/039	L2SP
	14.09	Landsat 8	6.32	142/038	L2SP
2012	16.06	Landsat 7	2.00	141/039	L2SP
	04.09	Landsat 7	1.00	141/038	L2SP
	27.09	Landsat 7	0.00	142/038	L2SP
	27.09	Landsat 7	2.00	142/039	L2SP
2006	31.05	Landsat 7	7.00	141/038	L2SP
	31.05	Landsat 7	3.00	141/039	L2SP
	27.09	Landsat 7	1.00	142/039	L2SP
	27.09	Landsat 7	0.00	142/038	L2SP
2001	03.07	Landsat 5	2.00	142/038	TM_L2SP
	21.09	Landsat 5	0.00	142/039	TM_L2SP
	22.09	Landsat 7	0.00	141/039	L2SP
	22.09	Landsat 7	0.00	141/038	L2SP

and the 1:250,000 Geomorphology-Ecology Map of Cuomai Area were used, both obtained from the Bureau of Land and Resources of Tibet Autonomous Region and digitized thereafter.

2.3 | Grassland type extraction

Reports from the Tibetan Plateau Comprehensive Scientific Expedition Team (1988), the Editorial Committee of the Vegetation Map of China (2007), the Tibet Autonomous Region Bureaus of Land Administration and Animal Husbandry (1994), and our field surveys collectively indicate that topography, moisture, and heat are the primary factors affecting vegetation zonation on the plateau. In this study, the primary topographic variables selected include elevation, slope, aspect, and ruggedness, which have been extensively utilized in analyses of altitudinal vegetation zoning (Pang et al., 2012; Shen et al., 2000) and ecological research (Korner, 2007; Xu, 2016). Given that intrazonal vegetation is distributed in waterlogged depressions, the depth of depressions was chosen as the hydrological variable. The heat variable was represented by Fractional Vegetation Cover (FVC), derived from the Normalized Difference Vegetation Index (NDVI), which reflects the level of solar radiation utilization by plants (Wang et al., 2003). Leveraging the overlay analysis function of ArcGIS 10.6, grassland landscape types were extracted based on the corresponding thresholds of habitat factors in Table 2 and depicted in Figure 2. Subsequently, the classification results were evaluated as follows: (1) Using the "Create Random Points" tool in ArcGIS, 50 randomly generated points were uniformly distributed for each grassland type; (2) 250 sample points (Figure 1) were overlaid onto the "1:250,000 Soil Type Distribution Map of Coqen County" and the "1:250,000 Geomorphology-Ecology Map of Cuomai Area," and vegetation attributes at each point individually assessed to determine the accuracy of each type; and (3) A confusion matrix was established, and the kappa coefficient was calculated to assess consistency. It is typically recommended that the sample size aligns with the actual total, and the number of training samples for remote sensing image classification should be 10–30 times the number of spectral bands, that is, "the larger, the better." (Foody & Mathur, 2006) The classification results presented in this study do not represent the actual extent of each type, and there is no direct correlation between them. The purpose of the extraction process is not to capture the entire geographical distribution of each grassland type but rather to focus on core areas. Therefore, the quantity of samples is not of utmost importance; instead, emphasis should be placed on ensuring that the sample points are uniformly distributed within the core habitats of each type. Computational analysis showed an overall accuracy of 78.4% and a Kappa coefficient of 0.6875, indicating a "substantial" agreement between the classification values and the true values of the sample points (Landis & Koch, 1977), indicating a relatively high level of classification accuracy.

2.4 | Landscape indices

A grassland type map is a qualitative representation of spatial data pertaining to grasslands, with landscape indices emerging as the most suitable tools for analyzing such data (Wu, 2000). It is essential to select a landscape index that avoids high correlation (Li & Reynolds, 1994). Baude and Meyer (2023) employed three indicators, namely "shape conditions", "diversity" and "fragmentation", to analyze changes in two German cities over a span of 168 years, establishing a link between land use, landscape structure, and ecosystem services. Du et al. (2023) designed a Landscape Ecological Risk Index (LERI) and established a multivariate linear equation using risk area, landscape fragility index, landscape isolation, and landscape dominance to analyze land cover changes across the Yellow River basin and assess its ecosystem stability. The theoretical foundation of these landscape indices lies in the physical properties of spatial objects. Physical features exhibit significant spatial randomness, with basic attributes including geographical location, area, shape, and distance, all independent of each other. Thirteen landscape indices were selected for this study based on the basic attributes of spatial variables (Table 3) to conduct a spatial–temporal analysis of alpine grasslands, focusing on grassland quantity, structural changes, and habitat fragmentation in the Zhari Namco basin. Calculation tools were sourced from FRAGSTATS v4.2.1.603.

2.5 | Analysis of land cover transfer

Transfer analysis can assist in determining the primary direction and magnitude of transfer among different grasslands and detecting changes in landscape patterns at the community scale. Land cover transfer analysis, based on remote sensing classification technology, requires obtaining clear optical features and spatial boundaries of objects, including each pixel in the study area. This study extracts core habitat areas of the communities while simultaneously generating large non-core habitat areas and water bodies (Figure 2), all of which hold significant ecological importance. The upper elevation threshold in the study area is set at 5280 m for the alpine sparse vegetation zone and the permanent snow zone above it,

TABLE 2 Habitat factor thresholds for various types of plant communities in the Zhari Namco basin.

Type	Terrain				Hydrology	Heat
	Elevation (m)	Slope (°)	Aspect (°)	Relief (m)	Depth of depression (m)	FVC[a]
1. *Carex* swamp meadow	It is characterized by perennial *Carex*-type rhizomatous herbaceous species and miscellaneous grass species. It has a very small distribution area and is typically on lakeshores with abundant water sources. The percent grassland cover[b] ranges from 70% to 80%					
	4418–4472; 4487–4505; 4607–4651; 4655–4681; 4715–4766; 5143–5200	0.2–7.2	–	1–10	1–8	0.4454–0.7754
2. *Stipa purpurea* steppe	It is a perennial bunchgrass type. It is found on wide plateaus, gentle slopes, broad valleys, lake shores, and lake plains, at elevations ranging from 4300 to 5000 m. It features alpine meadow soil, with grassland cover percentage ranging from 20% to 45%.					
	4671–4876	0.9–8.5	112.5–247.5	3–16	–	0.1500–0.2398
3. *Stipa purpurea* + *Carex moorcroftii* steppe	It is distributed on sunny slopes, ridges, and plateaus in mountainous areas, at elevations ranging from 4800 to 5200 m. It is located above the altitudinal zone dominated by *Stipa purpurea* as the sole dominant species, with alpine meadow soil and a small amount of meadow soil. The grassland cover percentage ranges from 20% to 50%.					
	4455–4620; 4903–5147	0–9	112.5–247.5	2–23	–	0.0949–0.1450
4. *Kobresia pygmaea* meadow	It is a cold-tolerant, perennial herbaceous grassland type. It is patchily distributed on relatively moist, shady slopes in alpine areas. It is found at elevations ranging from 4800 to 5600 m and features alpine meadow soil, with grassland cover percentages ranging from 70% to 95%.					
	4850–5280	1.5–20	0–67.5; 292.5–360	4–32	–	0.2040–0.2869
5. *Kobresia littledalei* meadow	It is an endemic grassland type in the Qinghai–Tibet Plateau, occurring in non-saline and non-well-drained river floodplains, in the phreatic zone at the margins of alluvial fans, and in ice-affected depressions. It is found at elevations ranging from 4300 to 5100 m and features swampy meadow soil, with grassland cover percentages ranging from 50% to 95%.					
	4473–4486; 4506–4606; 4682–4714; 4767–5200	0–7.3	–	3–10	5–14	0.4454–0.7754

Note: The threshold values for each factor were determined according to previous reports of Tibetan Plateau Comprehensive Scientific Expedition Team (1988), Editorial committee of vegetation map of China (2007) and Tibet Autonomous Region Bureaus of Land Administration and Animal Husbandry (1994) and multiple field surveys.

[a]Dimensionless unit, Selection of the range of thresholds for fractional vegetation cover was based on the values of percentage grassland cover, aimed at not only facilitating differentiation between grassland types but also maintaining vegetation cover.

[b]Percentage grassland cover was determined using plot surveys according to a literature report of Editorial committee of vegetation map of China (2007).

which are unrelated to grazing. Therefore, the height range for transfer analysis is set at ≤5300 m. Additionally, the water extraction method involves using the normalized difference water index (NDWI) in ENVI 5.6, with the results depicted in Figure 10.

3 | RESULTS

3.1 | Changes in area

The largest grassland type in terms of CA across different periods was the *K. pygmaea* meadow (1888–2303 km^2), followed by the *S. purpurea* steppe (1136–1468 km^2) (Figure 3). The area of the *K. littledalei* meadow and the *S. purpurea* + *C. moorcroftii* steppe fluctuated between 257–303 and 46–294 km^2, respectively. Although the *Carex* swamp meadow was sampled across seven different elevation ranges, its area was the smallest due to its limited geographical distribution. Despite the *S. purpurea* steppe being the zonal vegetation in the study region, its sampled area was not the largest. Notably, the *S. purpurea* + *C. moorcroftii* steppe was only about 46 km^2 in 2021, even smaller than the area of *Carex* swamp meadow in any period, which is inconsistent with reality. Unlike land use or land cover classifications, there are no definitive values for the area of each community type at any given period, and accurate spectral

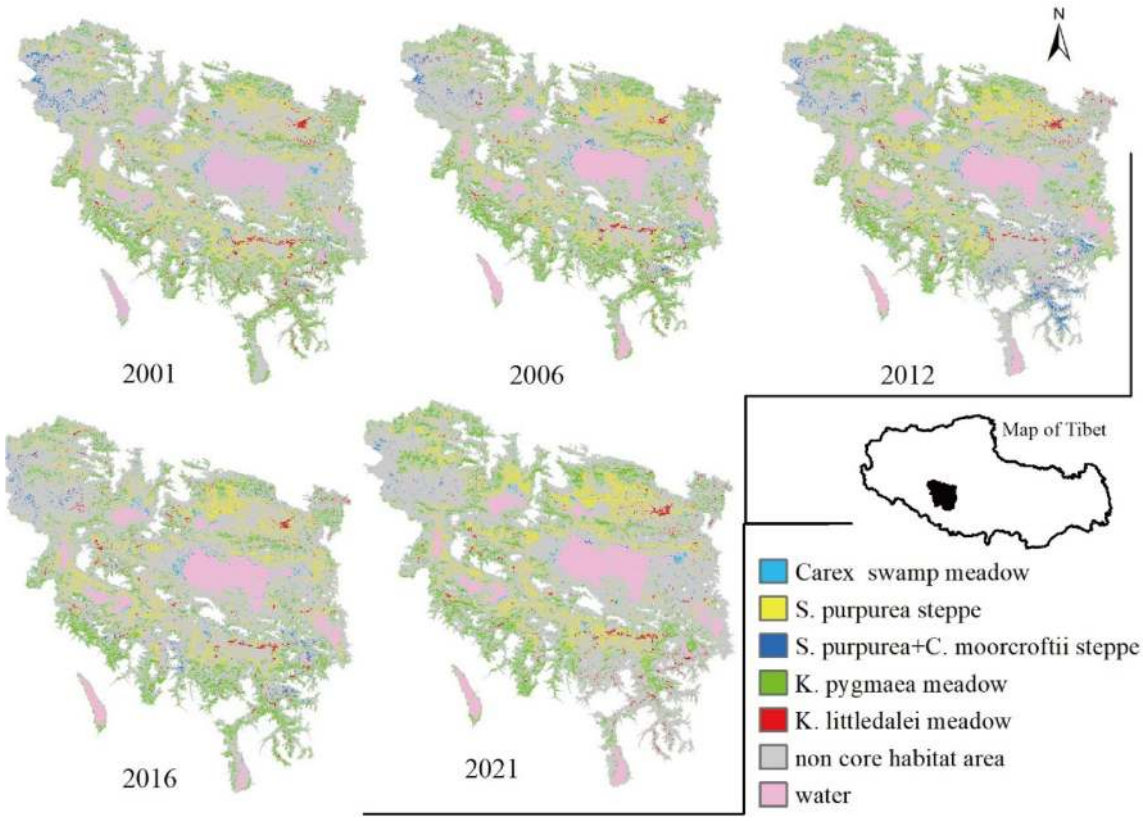


FIGURE 2 Plant community types of the alpine grasslands in the Zhari Namco basin, 2001–2021.

characteristics of the community cannot be determined. This makes the extraction and classification of the entire domain impossible. Therefore, sampling results are subject to strict habitat factor threshold constraints, rather than direct representations of the actual area of the grassland type.

The area growth rate serves as a dimensionless metric, suitable for comparing the degree of area changes (Figure 4). In this study, slight area changes were categorized within the range of $\in \pm 20\%$ in each period, moderate area changes as falling within the range of $\in (\pm 20\%, \pm 40\%)$ in at least one period, and dramatic area changes as $\in > 40\%$ in at least one period. According to these definitions, the following observations were made: (1) between 2001 and 2006, *S. purpurea* steppe and *K. pygmaea* meadow experienced slight increases in the area (<20%), while *S. purpurea* + *C. moorcroftii* steppe exhibited a moderate decrease (>20%). The overall grassland landscapes witnessed a 7.19% increase, marking the highest 5-year increase over the 20-year period. (2) From 2006 to 2012, *S. purpurea* + *C. moorcroftii* steppe saw a notable increase of 116.54%, whereas *S. purpurea* steppe and *K. pygmaea* meadow only decreased by 3.8% and 24.7%, respectively. The entire grassland landscape experienced a 12.2% decline, marking the highest five-year decrease over the 20-year period. (3) Although *S. purpurea* + *C. moorcroftii* steppe experienced a cumulative decrease of approximately 112% over the two periods, the slight increase in the area of *S. purpurea* steppe (22.9% in 2021) and *K. pygmaea* meadow (9.8% in 2016) still had a positive impact on the total area (0.7% in 2016; 2.5% in 2021). These findings suggest that *S. purpurea* steppe and *K. pygmaea* meadow had a significant impact on the entire grassland landscape, and their minor changes in area growth rate could affect the overall grassland landscape.

3.2 | Changes in community structure

3.2.1 | Patch density

In terms of grassland types, three levels of differences are observed (Figure 5). First, the C_PD values of *S. purpurea* steppe and *K. pygmaea* meadow were significantly higher than those of the other community types, indicating relatively high patch dispersion. Both grasslands showed slight fluctuations and increased over the 2001–2016 period, reaching their maximum densities in 2016 at 11.47 and 13.28 patches/km^2, respectively. However, by 2021, these values rapidly decreased to slightly above the 2001 level, at 9.41 and 12.31 patches/km^2, respectively. Second,

TABLE 3 Introduction and function of 13 landscape indices.

Dimension	Indices	Abbreviations	Formula	Description and comments
Quantity	Class/total area	CA TA	$CA = \sum_{j=1}^{n} a_{ij} \times 10^{-6}$ (1) $TA = A \times 10^{-6}$ (2) CA>, TA>0. a_{ij}, area (m^2) of patch ij; A, km^2, the sum of the areas of all patches.	CA and TA represent the sum of the areas of all patches corresponding patch class (C) or Total (T) landscape.
Structure	Class/total patch density	C_PD T_PD	$PD = n_i/A$ (3) PD > 0, number/km^2. n_i, number of patches in the class i or total; A, as Formula (1) and (2).	The larger value, the higher degree of habitat fragmentation and the lower the more complete the landscape pattern.
	Coefficient of variation of patch area	CA_CV TA_CV	$ACV = \frac{SD(a_{ij})}{MN(a_{ij})} \times 100\%$ (4) A_CV≥1, dimensionless. a_{ij}, area (m^2) of patch ij; SD (a_{ij}), the standard deviation of the patch area in the class or total; MN (a_{ij}), the mean of the patch area in the class or total.	The larger value, the more discrete the patch size of class or total. The smaller, the more uniform. When the means of multiple variables are not equal.
	Coefficient of variation of patch shape	CS_CV TS_CV	$SCV = \frac{SD(S_{ij})}{MN(S_{ij})} \times 100\%$ (5) $S_{ij} = \frac{0.25P_{ij}}{\sqrt{a_{ij}}} \times 100\%$ (6) S_CV≥1, dimensionless. SD (S_{ij}), the standard deviation of S_{ij}; MN (S_{ij}), the mean of S_{ij}; $S_{ij} \geq 1$, m/m^2, the deviation of patch ij perimeter from that of a square with the same area; P_{ij}, m, patch perimeter; a_{ij}, m^2, as formula (1).	The lager value, the greater unevenness in patch shape. It is used to reflect the degree of shape variability and complexity among patches.
Habitat fragmentation	Patch connectivity	C_PX T_PX	$PX = \sum_{i=1}^{N} \left[\frac{A(i)/NND(i)}{\sum_{i=1}^{N} A(i)/NND(i)} \right]$ (7) PX ∈ (0, 1], dimensionless. A (i), m^2, area of patch i in class or total; NND (i), m, the minimum distance from patch i to its neighboring patches needed to specify a distance threshold by user; N, number of patches.	The larger value, the higher tendency for the patches to aggregate. It is suitable for describing the degree of connectivity between patches of the same type (Li, 1989).
	Dominance	D	$D = H_{max} + \sum_{i=1}^{N} P_k ln(P_k)$ (8) D >0, dimensionless, the difference between H_{max} and the actual value. H_{max}, the maximum value of the diversity index; P_k, the probability of patch class k occurring in the landscape; N, the total number of patch types.	A larger D value indicates the presence of one or a few dominant patch types.
	Evenness	E	$E = \frac{-\sum_{i=1}^{N} P_k ln(P_k)}{ln(n)}$ (9) $E \leq 1$, dimensionless. P_k and N, as formula (8).	The closer the value of E to 1, the higher the degree of uniformity of landscape patch distribution.
	Simpson's diversity	H′	$H' = 1 - \sum_{k=1}^{N} P_k^2$ (10) H′∈[0, 1), dimensionless. P_k and N, as formula (8).	A larger value indicates an increasing complexity in the composition of the landscape structure. D, E, and H' are suitable metrics of the uniformity of area distribution and often used together to reflect the structural complexity at the landscape scale.

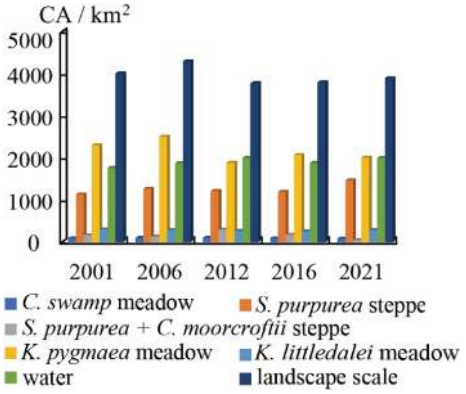


FIGURE 3 Patch area statistics of both type and landscape scales, 2001–2021.

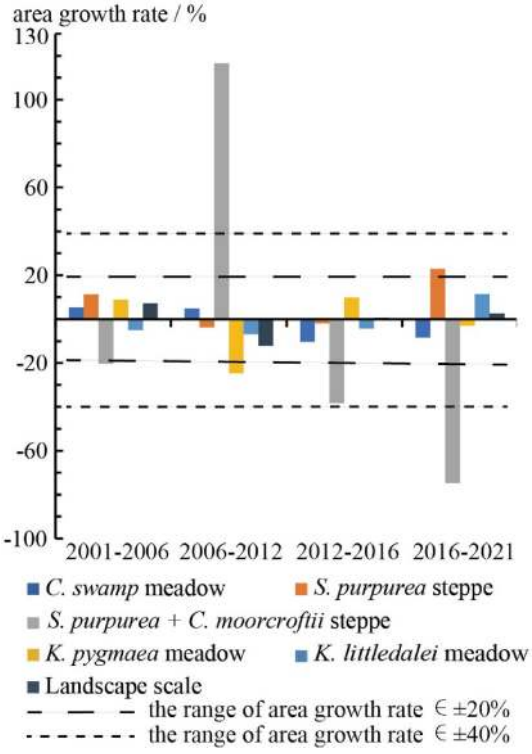


FIGURE 4 Area growth rate for both type and landscape scales, 2001–2021.

in contrast, *Carex* swamp meadow and *K. littledalei* meadow consistently exhibited the lowest patch densities (1–2 patches/km^2) throughout the 20-year period, with minimal fluctuation. Third, *S. purpurea* + *C. moorcroftii* steppe exhibited noticeable fluctuations, characterized by an "aggregated-dispersed-aggregated" pattern. The patch densities were relatively high from 2006 to 2016 at 4.03 and 3.96 patches/km^2, respectively. This was followed by a decrease to 1.19 patches/km^2 in 2021, which is lower than that of *K. littledalei* meadow but similar to that of *Carex* swamp meadow. In reality, the spatial distribution

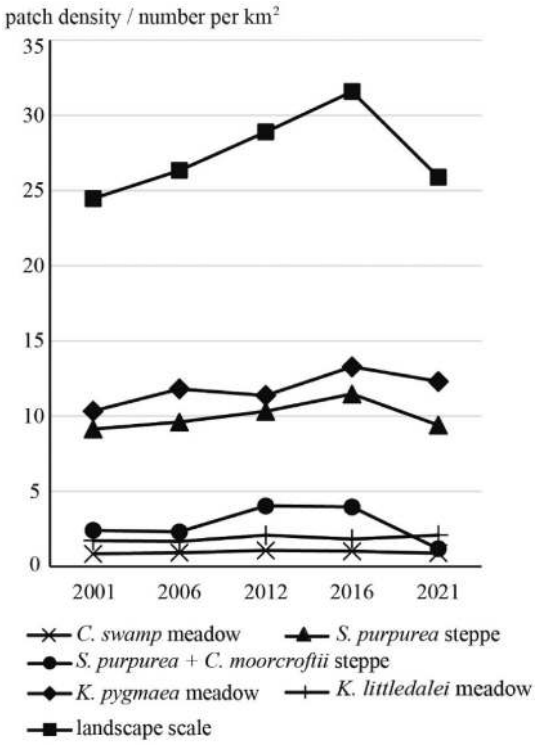


FIGURE 5 Patch density for both type and landscape scales, 2001–2021.

of the five community types mentioned above is continuous, with the hydrothermal combination mainly constrained by consistent plateau zonation. The main factor contributing to differences in patch density is grazing practices in different communities.

In addition, the temporal trend of T_PD for the entire grassland landscape mirrored that of C_PD for the *S. purpurea* steppe. It increased from 2001 to 2016, reaching the maximum value in 2016 at 25.89 patches/km^2, followed by a rapid decrease to slightly above the baseline value in 2021 at 24.46 patches/km^2. Similarly, the fluctuation trends in TA_CV (Figure 6f) and TA_SV (Figure 7f) also closely resembled those of *S. purpurea* steppe. However, it is worth noting that the T_PD values were significantly several times higher than the corresponding C_PD values, ranging from approximately 24 to 32 patches/km^2 (Figure 5), which is about twice that of *K. pygmaea* meadow and three times that of *S. purpurea* steppe.

3.2.2 | CVs of patch area and patch shape index

The CA_CV of *Carex* swamp meadow (Figure 6a) from 2001 to 2016 was consistently lower by at least 200 compared to the other grassland types, then increased to nearly 800 by 2021, reaching a level comparable to that of

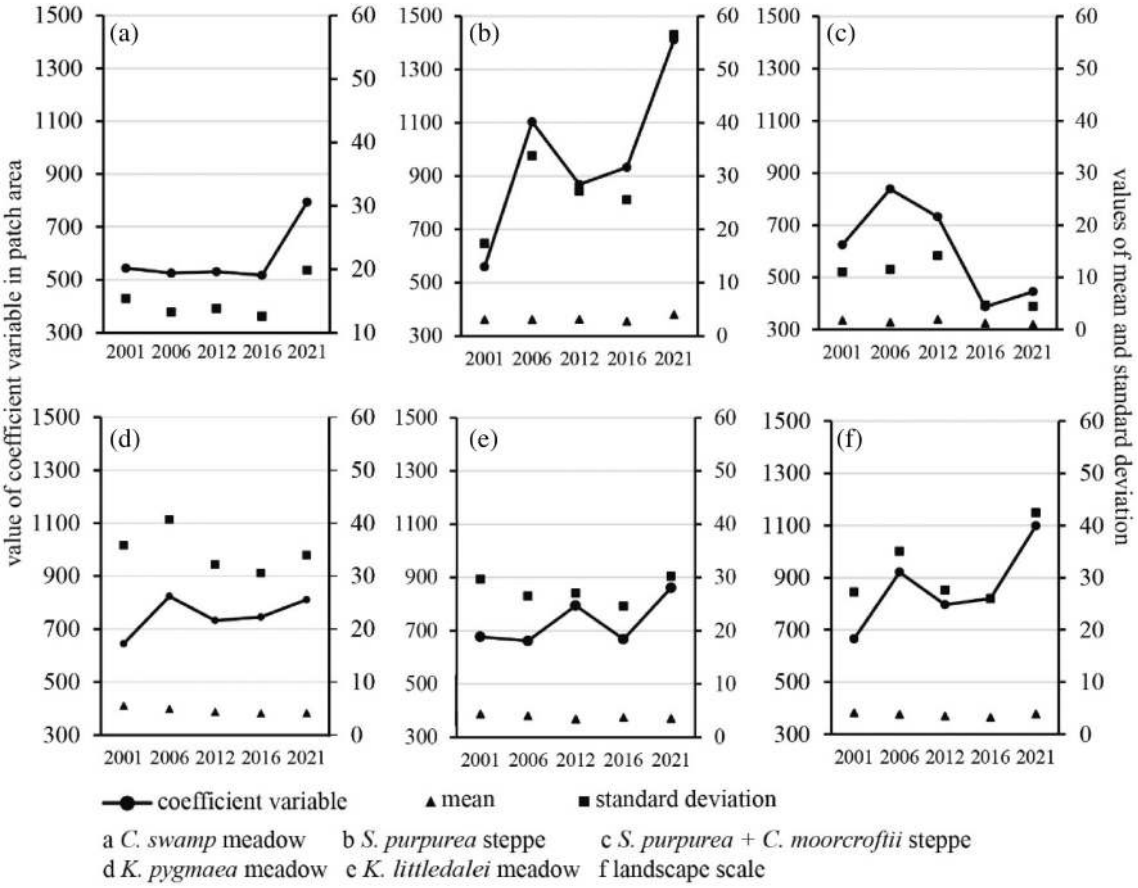


FIGURE 6 Coefficient of variation in patch area for both type and landscape scales, 2001–2021.

other communities in the first 5 years. However, its Cs_CV (Figure 7a) only shows a minimal increase in 2006 and 2021. This can be attributed to the significant increase in patch area differences after 2016, while the patch shape remained unchanged. *K. littledalei* meadow exhibits a similar pattern, with its patch area fluctuating over the 20 years within the range of CA_CV ∈(700, 900), yet the patch shape remains consistent. When considered alongside Figure 5, it becomes evident that over the long time series, patches in both grasslands remain aggregated, with no significant change in patch shape, indicating a stable community structure.

Comparing *K. pygmaea* meadow and *K. littledalei* meadow, the fluctuation range of CA_CV for both (600–800) (Figure 6d,e) is similar, with the former slightly larger than the latter (∼50 >40) (Figure 7d,e). Essentially, this indicates that over the past 20 years, the degree of change in patch area is similar for both types, while the patches in the *K. pygmaea* meadow exhibit a more complex in shape. However, complexity in shape does not necessarily indicate a more stable structure. As depicted in Figure 5, the patch density of the *K. pygmaea* meadow is approximately 10 times that of the *K. littledalei* meadow, and the difference between the mean and standard deviation of the patch area is also significantly larger (Figure 6d,e). In other words, at the type level, the patches within *K. pygmaea* meadow are notably dispersed, with the size of the patches being highly random, indicating an unstable community structure. The complexity of patch shapes in this community still stems from the topographical factors of its habitat, which are more pronounced compared to those of the *Carex* swamp meadow and the *K. littledalei* meadow.

The most significant changes were observed in *S. purpurea* steppe and *S. purpurea* + *C. moorcroftii* steppe. The former experienced a significant fluctuating increase and reached its peak in 2021 (559–1412; 0.45–0.57) (Figures 6b and 7b), suggesting a tendency towards dispersed community structure. In contrast, the latter showed a significant fluctuating decrease (838–445; 0.43–0.31) (Figures 6c and 7c), leading to increased aggregation. However, during the periods 2006–2012 and 2012–2016, *S. purpurea* steppe showed the most stable state, as evidenced by the decreased differences between the mean and standard deviation (Figures 6b and 7b). In other words, its patch size increased while the deviation from a square shape decreased. On the other hand, *S. purpurea* + *C. moorcroftii* steppe served as a transitional type from

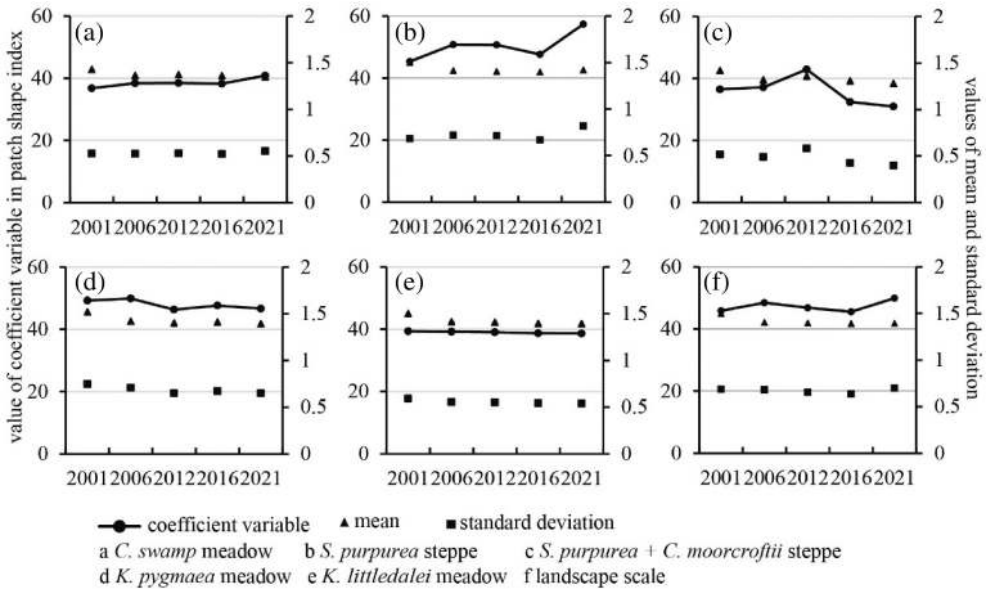


FIGURE 7 Coefficient of variation in patch shape index for both type and landscape scales, 2001–2021.

S. purpurea steppe to *C. moorcroftii* meadow and accounted for a small proportion of the altitudinal zones. It bordered the lake area and covered its surroundings at elevations ranging from 4455 to 4620 m and 4903 to 5147 m, where favorable hydrological conditions likely played a dominant role in improving its community structure.

3.3 | Changes in habitat fragmentation

3.3.1 | Patch connectivity

Field investigations revealed that alpine grasslands in the study area were widely distributed, and the dominant vegetation community types exhibited no significant changes within areas spanning tens of square kilometers. To analyze the temporal and spatial variation characteristics of PX, starting with the mean NND (nearest-neighbor distance) of the entire grassland landscape in 2001, seven connectivity distance thresholds were set at 243, 500, 1000, 1500, 2000, 2500, and 3000 m. Calculations of C_PX and T_PX values were performed for each threshold and compared through mapping (Figure 8). Similar to the CA and C_PD, the changes in C_PX also exhibit three levels of differences. Initially, regardless of the periods, as the connectivity distance threshold increased, the C_PX values ranging from 0.0053 to 0.3145 for both *S. purpurea* steppe and *K. pygmaea* meadow were significantly smaller than those for other grassland types and consistently low across all five periods. This indicates that the long-term habitat fragmentation levels for both are consistently higher compared to others. Second, when the C_PX thresholds of *K. littledalei* meadow were ≤1000 m, no temporal differences were observed, similar to the two former types; for thresholds ≥1500 m, not only did the C_PX values increase, but significant temporal differences were also evident. However, its C_PX values ranging from 0.0199 to 0.3964 are only slightly higher than those of the two former types, without significant changes in community aggregation. Third, the C_PX values of both *Carex* swamp meadow and *S. purpurea* + *C. moorcroftii* steppe varied with time, regardless of the connectivity distance thresholds. The temporal response of the former is not obvious, indicating a long-term presence in a relatively well-aggregated state. The latter exhibits temporal variations. At the threshold of 3000 m, the connectivity of *S. purpurea* + *C. moorcroftii* steppe was around 0.76 over the period 2001–2006, then significantly dropped to the lowest value of 0.49 in 2006–2016. This indicates that the habitat fragmentation levels fluctuate between decreasing and increasing. One noteworthy point is that the continuous decrease in CA_CV and CS_CV for *S. purpurea* + *C. moorcroftii* steppe during the period of 2006–2016 indicates a shift in community structure towards aggregation. While its C_PD and C_PX showed opposite trends, with a continuous increase from 2006 to 2012 to reach its highest value, and a continuous decrease from 2012 to 2016 to reach its lowest value over the 20-year period, only showing a consistent change towards community structure aggregation until 2021. It appears that there is a lag of approximately 10 years in the transition of community habitat fragmentation levels.

3.3.2 | Simpson's diversity

Landscape diversity reflects the temporal changes of grassland structure across the entire landscape. As shown in Figure 9, dominance experienced a slight increase from −0.29 to −0.25 during 2001–2006, followed by a

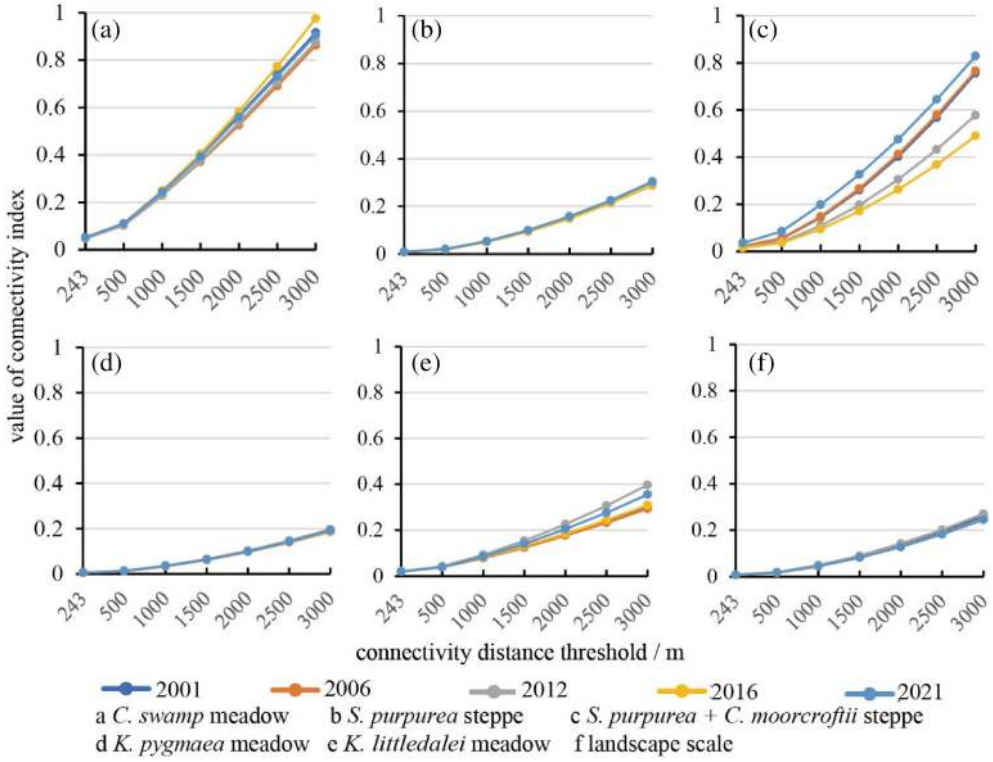


FIGURE 8 Connectivity index for both type and landscape scales, 2001–2021, when setting connectivity distance thresholds to 243, 500, 1000, 1500, 2000, 2500, or 3000 m.

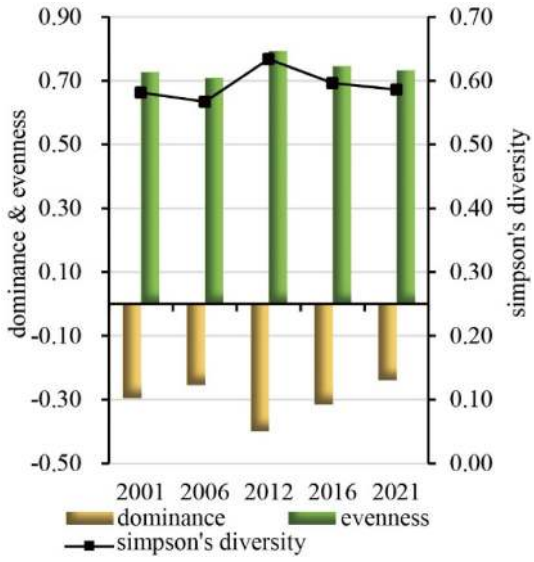


FIGURE 9 Variation in dominance, evenness, and Simpson's diversity on the landscape scales, 2001–2021.

decline to its lowest value of −0.40 in 2012. Approximately a decade later, it consistently rose to −0.23 by 2021, marking the highest value in the past 20 years. Conversely, evenness showed a slight decrease in 2001 and 2006, followed by an increase in 2012, and a subsequent decrease in 2016 and 2021, exhibiting an opposing trend to dominance. These opposite temporal patterns indicate that in 2006, one grassland type became dominant while others degraded or disappeared, resulting in lower landscape stability compared to 2001. By 2012, the dominance of one grassland type reached its lowest level in the past 20 years, representing the most stable period of landscape structure recovery. In 2016 and 2021, dominant grassland types emerged again with higher evenness index values than those observed before 2012. This indicates a decrease in landscape stability since 2012, although it remained higher compared to the period before 2012. Simpson's diversity reached its peak in 2012 (0.63), further highlighting the temporal complexity trend in landscape structure. Around 2012, both landscape complexity and stability increased from 2001 to 2012 but decreased from 2012 to 2021.

3.4 | Characteristics of area transfer

Although the absolute value of the sampling area does not correlate with the actual area, the absolute value of the transfer area can reflect the direction and intensity of temporal and spatial changes. As shown in Figure 10, there have been two phases of increased area transfer over the past two decades, specifically during 2001–2006 and 2012–2016. By analyzing the annual livestock output values for Coqen County spanning from 2000 to 2020, followed by sampling at intervals based on community types, the average values of livestock output for the respective periods were calculated (Figure 11).

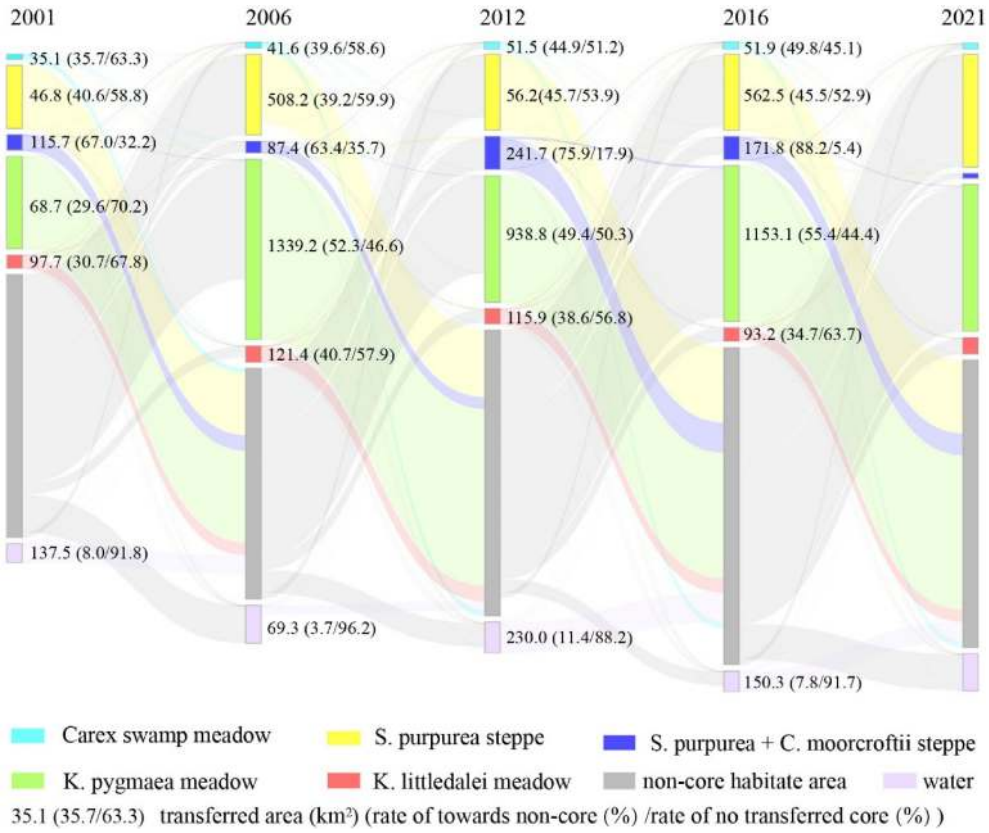


FIGURE 10 Transfer trajectory map of changing plant community core habitats, water regions and non-core habitats, 2001–2021.

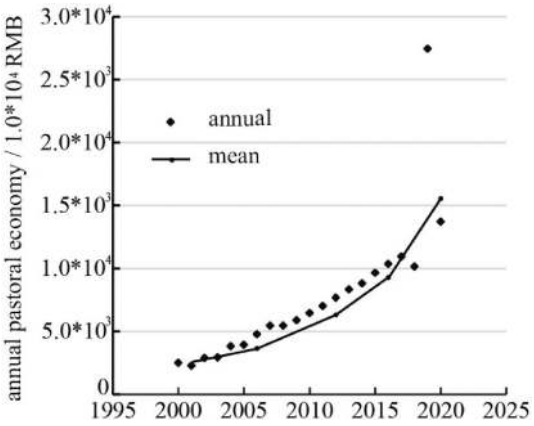


FIGURE 11 Scatter and line chart of pastoral economy annual output in Coqen County, 2000–2020 (data source: Tibet Statistical Bureau, 2001–2021).

The results reveal a consistent increase in livestock output over the past 20 years, with 2006 and 2016 serving as two pivotal years of increased production coinciding with the periods of enhanced transfer at the landscape scale. It is evident that the development of animal husbandry has initiated an adjustment mechanism in the alpine grassland community structure in the study area, leading to the spatial transfer of core habitat areas for dominant plant communities.

It also highlights two primary directions of transfer for all habitat types: one maintaining stability, while the other transitions to non-core habitat areas (Figure 10). *Carex* swamp meadow and *K. littledalei* meadow exhibit relatively balanced transfer amounts, but the proportion of the former's core habitat area converting to non-core increases in each period (35.7%, 39.6%, 44.9%, and 49.8%). In contrast, the latter maintains a higher proportion of unchanged core habitat areas (67.8%, 57.9%, 56.8%, and 63.7%). Both *S. purpurea* steppe and *K. pygmaea* meadow undergo the most significant transfers, predominantly towards non-core areas. However, in the case of *S. purpurea* steppe, more than 52% of its core habitat areas remain unchanged over the 20-year period, ranking it first among all the communities. As a zonal vegetation, the stable spatial distribution of core habitats indicates the stability of the entire ecosystem. Regarding *K. pygmaea* meadow, the transfer area reached 1339.2 km^2 in 2006–2012, nearly twice that of 2001–2006. Its second significant transfer occurred in 2016–2021, covering 1153.1 km^2, which is 1.2 times larger than that of 2012–2016. This temporal pattern precisely aligns with two pivotal points in the growth of the pastoral economy (Figure 11). Furthermore, the percentage of its core habitat area remaining unchanged in the directional transfer decreased from 70.2% in 2001–2006 to 46.6% in 2006–2012. This suggests that changes in the pastoral economy

around 2006 or intensified grazing have significantly impacted the core habitat area of the *K. pygmaea* meadow. Between 2012 and 2016, the transfer area of *S. purpurea* + *C. moorcroftii* steppe reached 241.7 km^2, 2.7 times larger than that between 2006 and 2012, and highly significant within the communities. Moreover, it experienced a high percentage of core habitat areas shifting to non-core, accounting for 63.4%, 75.9%, and 88.2% in 2006, 2012, and 2016, respectively. During this period of 2012–2016, a water area of 230 km^2 underwent a transfer, marking 3.3 times increase compared to the transfer between 2006 and 2012, and accounting for 11.8% of the total water area in 2012. Notably, 11.4% of this transfer was directed towards non-core areas, representing the most significant spatial expansion phenomenon in the 20-year period.

4 | DISCUSSION

4.1 | Habitat differences and community-scale responses

Zhang et al. (2020) and Liu et al. (2015) investigated the relationship between the seasonal variations in NDVI and different levels of grazing intensity in the alpine grasslands of the Tibetan Plateau. They suggested that while plant growth increased in most areas, it decreased in specific regions. Recent research on alpine meadows in the eastern and southeastern regions of the Qiantang Plateau, where *K. pygmies* dominates, indicates that sustained degradation of alpine meadows has been ongoing for 30 to 50 years due to climate change and overgrazing pressures. Without protective measures, certain meadows are at risk of disappearing within decades (Liu et al., 2018; Miehe et al., 2019). Despite focusing on similar research subjects and regions, these studies employed different ecological indicators and reached different conclusions. One of the primary issues is the ambiguous delineation of the alpine grassland ecosystem on the Qinghai–Tibet Plateau. Although the Qiantang Plateau generally experiences a cold and arid monsoon continental climate, the grasslands north of the Gandis—Nyen Chen Tangela Mountains exhibit distinct plateau zonation characteristics. The transitional zone between the western part of southeastern Qiantang and the alpine steppe of the plateau, represented by the wide valley basin in this study, features alpine meadow steppe occupying both horizontal and vertical geographic space. This zone exhibits unique hydrothermal conditions, plant composition, and natural economic characteristics that differentiate it from the alpine steppe. In the 1990s Tibet Land Resources Survey, it was classified separately as a distinct grassland type. Environmental factors predominantly shape the structure of these ecosystems, with evidence of ecosystem changes discernable only at the community level.

Zhou et al. (2006) conducted a study on the alpine meadow at the Hai Xi monitoring station in the northern Qinghai–Tibet Plateau, spanning from 1957 to 2000. They used three indices: Net Primary Productivity, annual precipitation, and annual average temperature. They concluded that the *K. humilis* meadow ecosystem, undisturbed by human activities, exhibits high stability. As the plateau zonation characteristics extend towards the interior of Qiantang, the dominant meadow community in the study area transitions to the more cold-tolerant *K. pygmaea* meadow, originating from the upper and middle parts of the mountain. Particularly, these meadows thrive on shaded and semi-shaded slopes with minimal grazing impact, making them a valuable reference for understanding stability changes in the alpine grassland ecosystem of southern Qiantang.

Other communities exhibit stability either superior to or comparable to that of the *K. pygmaea* meadow, but notable differences exist in the level of community structure aggregation. First, the stability of the *S. purpurea* steppe is consistent with that of the *K. pygmaea* meadow, but the degree of community structure changes is significantly higher. This significant difference likely stems from increased grazing intensity from 2016 to 2021 (Figure 11). Second, both in terms of community structure aggregation and stability, the *S. purpurea* + *C. moorcroftii* steppe surpasses the *K. pygmaea* meadow, exhibiting the best resilience. Positioned within the primary economic activity area of Coqen county, this ecosystem experiences strong human influence. However, inconsistencies in the timing of the three indices, T_PD, TA_CV, and T_PX, also suggest a significant lag effect under external pressures. Third, the *Carex* swamp meadow and *K. littledalei* meadow represent typical, habitat-restricted, and cryptic plant communities, serving as crucial forage resources for local herding. Compared to the *K. pygmaea* meadow, the former exhibits exceptional community structure aggregation and significant stability unaffected by time, seemingly resilient to external pressures. Conversely, the latter exhibits community characteristics very similar to those of the *K. pygmaea* meadow. However, grazing pressure on the *K. pygmaea* meadow is lower, indicating better carrying capacity for livestock.

4.2 | The impact of hydropower infrastructure construction on the communities

The policies proposed during the Fourth Tibet Work Symposium in 2001 emphasized the development of

animal husbandry, promoting income growth for herders, and improving infrastructure in pastoral areas. In Tibet's northern pastoral area, water serves not only as a crucial ecological element but also as a crucial resource for production and livelihood. Since 2010, Coqen County has initiated the construction of power stations along major rivers and the renovation of river channels, while simultaneously improving canal construction for artificial grass planting and irrigation projects. By 2022, major river engineering projects, including projects along the Coqen Zangbo River in Coqen Town, Chiaju Zangbo River in Quluo Town, Langrong River in Daxiong Town, and Sangwu Zangbo River in Cishi Town, had been completed (Cang, 2022). These initiatives led to a significant increase in water area since 2006, peaking in 2012 and showing no decline until 2021 (Figure 3). A comparison with the findings of Simpson's diversity index (Figure 9) suggests that the increase in water area from 2001 to 2012 promoted the complexity of landscape-level structures, leading to landscape process stability. However, from 2012 to 2021, the diversification of water resource utilization improved residents' well-being but disrupted the internal water cycle of the ecosystem, resulting in a decline in landscape diversity. Water is a crucial component of the alpine grassland ecosystem, effectively influencing communities sensitive to hydrological changes. In *Carex* swamp meadow habitats, groundwater saturation leads to the progressive expansion of waterlogged areas. Conversely, in *K. littledalei* meadow habitats, groundwater levels remain constant, resulting in minimal changes in waterlogged areas. The *S. purpurea* + *C. moorcroftii* steppe serves as a focal point for production activities in Coqen County. Over the course of more than a decade, continuous hydraulic infrastructure construction has established a spatial configuration of water resources targeting electricity usage and pasture management. This has facilitated surface runoff regulation during dry and flood periods, significantly increasing water resources in the habitat area and directing them towards enhanced utilization areas. Despite a gradual increase in grazing intensity over time, the ecological service function of this community remains robust, with its structure exhibiting a trend towards aggregation and ecosystem stability. The responses of these communities indicate that regional water resource regulation measures support the development of animal husbandry in lakeside areas, representing the only sustainable development region in the Qiangtang Plateau. In the future, efforts should be made to strengthen habitat change monitoring, providing scientific support for local social development initiatives.

4.3 | The impact of grazing intensity on the communities

Since 2001, policies have been instrumental in driving the development of the pastoral economy in Coqen County. Although precise livestock numbers over the past 20 years are unavailable, the value of the pastoral economy directly reflects the grazing intensity (Figure 11). According to the Intermediate Disturbance Hypothesis, moderate grazing can promote community biodiversity, while overgrazing tends to diminish it (Whittaker, 1953). The *S. purpurea* steppe, serving as the largest seasonal pasture and an indicator of overall grassland changes, indicates that grazing intensity remained moderate from 2001 to 2016 but transitioned to overgrazing from 2016 to 2021. Currently, in the Qiangtang alpine plateau, there is a lack of industrialized lambing and rearing technologies, and the development of the pastoral economy mainly relies on expanding pasture areas. Although the *K. pygmaea* meadow is minimally affected by grazing, the areas converted from non-core to core areas in each period amount to 882.6, 716.5, 1097.9, and 1070.9 km^2, respectively, constituting 35.2%, 37.9%, 53%, and 53.3% of the total area of this community during the same timeframe (Figure 10). Expanding grazing areas have resulted in the continuous discretization of the community structure, indicating excessive grazing intensity at each stage. Zhang et al. (2020) compiled grazing intensity data from summer grazing experiments in northern Tibet, categorizing Coqen County as having moderate grazing intensity (3–5 sheep units/hm^2), while other counties in Ali City had light grazing intensity (1–3 sheep units/hm^2). However, there are differences in the carrying capacity of community habitats, and while moderate grazing intensity may hold statistical significance, it lacks practical relevance in guiding pasture management. Wang et al. (2004) studied the biomass of grassland communities in the hinterland of the Qinghai–Tibet Plateau and highlighted that different community types experience varying degrees of degradation under the same pastoral economic pressure. Therefore, the most urgent measure is to reassess grazing intensity in each period and formulate policies for pasture zoning management.

5 | CONCLUSION

The most reliable method for analyzing grassland plant community structure is through plot surveys. However, conducting plot surveys in vast alpine areas, such as the research region spanning thousands of square kilometers, is nearly impossible. Although remote sensing imagery

can provide land cover information at large temporal and spatial scales, conducting basic ecological analysis, such as assessing composition, structure, and traits, becomes challenging when dealing with objects exhibiting high spectral similarity at the same time. Over hundreds to thousands of years, various plant community types in the Zhari Namco basin have adapted to diverse alpine habitat conditions, forming unique grassland landscape patterns. Although the spatial distribution of each type undergoes temporal changes under the influence of natural and human factors, the core distribution areas of dominant plant communities are expected to maintain habitat stability. This raises a crucial question: how can these core areas be identified? A combination of prior knowledge, field surveys, and vegetation spectral information provides an effective approach. The method used in this study to classify grassland plant communities is similar to the ecological research method of selecting a target sample plot, that is, sampling the same habitats at different time periods to observe the spatiotemporal variations of plant community types. This approach holds methodological implications for exploring the heterogeneity of alpine grasslands in the Qiangtang Plateau.

This study examines the extended temporal changes within the alpine grazing grassland system at the community level in southern Qiangtang, supplementing the understanding of landscape patterns and processes in the northern Tibetan grassland. The findings of this research support local pastoral management initiatives and inform the formulation of policies for social development. However, in high-altitude habitats characterized by slow material and energy cycles, further observation and assessment are necessary to understand the impact of economic development on habitats. Continuous efforts should be made to develop quantitative predictive models suitable for the northern Tibetan alpine grassland ecosystem.

AUTHOR CONTRIBUTIONS

All authors contributed to the study conception and design. Material preparation, data collection and analysis were performed by Lu Chen, Wei Zhang and Wenjie Li. The first draft of the manuscript was written by Lu Chen and all authors commented on previous versions. Huixin Zhang and Shijia Luo handled the new data collection and mapping of all the revised manuscript. All authors read and approved the final manuscript.

ACKNOWLEDGMENTS

We thank Giovanni Zurlini, Ph.D. for the Submission suggestion. We have great thanks to the editorial team and reviewers for their valuable comments. We also thank LetPub (www.letpub.com) for its linguistic assistance. This study was supported by the Key Project of Sichuan Province Key Laboratory of Philosophy and Social Sciences for Rural Land Use Monitoring and Assessing [NDZDS202402]; The Major Project of Sichuan Primary and Secondary School Teacher Professional Development Research Center, Grant/Award Number: PDTR2022-03; Chengdu Normal University high-level research project, Grant/Award Number: CS22XMPY0115; Chengdu Normal University talent introduction project, Grant/Award Number: YJRC2016-6. We also thank *Rui Li* and *Wenxi Chen* for their works during the first version of this article.

CONFLICT OF INTEREST STATEMENT

The authors have no relevant financial or non-financial interests to disclose.

DATA AVAILABILITY STATEMENT

The datasets generated during and/or analyzed during the current study are available from the corresponding author on reasonable request.

ORCID

Lu Chen https://orcid.org/0000-0002-3715-6821

REFERENCES

Baude, M., & Meyer, B. C. (2023). Changes in landscape structure and ecosystem services since 1850 analyzed using landscape metrics in two German municipalities. *Ecological Indicators*, *152*, 110365. https://doi.org/10.1016/j.ecolind.2023.110365

Chen, Z. K., & Lu, X. G. (2010). Comparison between the marsh wetland landscape patterns in the Zoige plateau for two periods. *Wetland Science*, *8*(1), 8–14. https://doi.org/10.13248/j.cnki.wetlandsci.2010.01.009

Cheţan, M. A., Dornik, A., & Urdea, P. (2018). Analysis of recent changes in natural habitat types in the Apuseni Mountains (Romania), using multi-temporal Landsat satellite imagery (1986–2015). *Applied Geography*, *97*, 161–175. https://doi.org/10.1016/j.apgeog.2018.06.007

Cang, L. (2022). *Significant achievements in Coqen water conservancy over the past decade. October 23, 2022*. http://www.xzcq.gov.cn/cgyw_1554/202210/t20221023_4412176.html

Dong, S., Shang, Z., Gao, J., & Boone, R. B. (2020). Enhancing sustainability of grassland ecosystems through ecological restoration and grazing management in an era of climate change on Qinghai-Tibetan plateau. *Agriculture, Ecosystems & Environment*, *287*, 106684. https://doi.org/10.1016/j.agee.2019.106684

Du, L., Dong, C., Kang, X., Qian, X., & Gu, L. (2023). Spatiotemporal evolution of land cover changes and landscape ecological risk assessment in the Yellow River Basin, 2015–2020. *Journal of Environmental Management*, *332*, 117149. https://doi.org/10.1016/j.jenvman.2022.117149

Editorial Committee of Vegetation Map of China, The Chinese Academy of Sciences. (2007). *Vegetation of China and its geographic pattern: Illustration of the vegetation map of the People's Republic of China (1:1 000 000)* (Vol. I). Geological Publishing House.

Filippa, G., Cremonese, E., Galvagno, M., Bayle, A., Choler, P., Bassignana, M., Piccot, A., Poggio, L., Oddi, L., Gascoin, S., Costafreda-Aumedes, S., Argenti, G., & Dibari, C. (2022). On

the distribution and productivity of mountain grasslands in the Gran Paradiso National Park, NW Italy: A remote sensing approach. *International Journal of Applied Earth Observation and Geoinformation*, *108*, 102718. https://doi.org/10.1016/j.jag.2022.102718

Foody, G. M., & Mathur, A. (2006). The use of small training sets containing mixed pixels for accurate hard image classification: Training on mixed spectral responses for classification by an SVM. *Remote Sensing of Environment*, *103*(2), 179–189. https://doi.org/10.1016/j.rse.2006.04.001

Kikuchi, T. (1990). ADCA analysis of floristic variation of plant communities in relation to micro landform variation in a hillside area. *Ecological Review*, *22*, 25–31. https://doi.org/10.2174/1567205011310040009

Kong, J. X., Zhang, Z. C., & Zhang, J. (2019). Classification and identification of plant species based on multi-source remote sensing data: Research progress and prospect. *Biodiversity Science*, *27*(7), 796–812. https://doi.org/10.17520/biods.2019197

Korner, C. (2007). The use of "altitude" in ecological research. *Trends in Ecology & Evolution*, *22*(11), 570–575. https://doi.org/10.1016/j.tree.2007.09.006

Landis, R. J., & Koch, G. G. (1977). The measurement of observer agreement for categorical data. *Biometrics*, *33*, 159–174.

Lewińska, K. E., Hostert, P., Buchner, J., Bleyhl, B., & Radeloff, V. C. (2020). Short-term vegetation loss versus decadal degradation of grasslands in the Caucasus based on cumulative endmember fractions. *Remote Sensing of Environment*, *248*, 111969. https://doi.org/10.1016/j.rse.2020.111969

Li, H. (1989). *Spatio-temporal pattern Anatysis of managed Forest landscapes: A simulation approach*. The Oregon State University.

Li, H., & Reynolds, J. F. (1994). A simulation experiment to quantify spatial heterogeneity in categorical maps. *Ecology*, *75*(8), 2446–2455.

Liu, S., Zamanian, K., Schleuss, P. M., Zarebanadkouki, M., & Kuzyakov, Y. (2018). Degradation of Tibetan grasslands: Consequences for carbon and nutrient cycles. *Agriculture, Ecosystems & Environment*, *252*, 93–104.

Liu, X. F., Zhu, X. F., Pan, Y. Z., Li, Y. Z., & Zhao, A. Z. (2015). Spatiotemporal changes in vegetation coverage in China during 1982-2012. *Acta Ecologica Sinica*, *35*(16), 5331–5342. https://doi.org/10.5846/stxb201404150731

Liu, Y. Q., Lv, C. H., Fu, B. J., & Yu, B. H. (2021). Terrestrial ecosystem classification and its spatiotemporal changes in China during last 20. *Ecologica Sinica*, *41*(10), 3975–3987. https://doi.org/10.5846/stxb202104130964

Ma, N. (2021). Comparison of variations in land surface evapotranspiration between typical alpine steppe and wetland ecosystems on the Tibetan plateau over the last four decades. *Advances in Earth Science*, *36*(8), 836–848. https://doi.org/10.11867/j.issn.1001-8166.2021.079

Miehe, G., Schleuss, P. M., Seeber, E., Babel, W., Biermann, T., Braendle, M., Chen, F., Coners, H., Foken, T., Gerken, T., Graf, H. F., Guggenberger, G., Hafner, S., Holzapfel, M., Ingrisch, J., Kuzyakov, Y., Lai, Z., Lehnert, L., Leuschner, C., … Wesche, K. (2019). The Kobresia pygmaea ecosystem of the Tibetan highlands: Origin, functioning and degradation of the world's largest pastoral alpine ecosystem—Kobresia pastures of Tibet. *Science of the Total Environment*, *648*, 754–771. https://doi.org/10.1016/j.scitotenv.2018.08.164

Ostendorf, B., & Reynolds, J. F. (1998). A model of arctic tundra vegetation derived from topographic gradients. *Landscape Ecology*, *13*, 187–201. https://doi.org/10.1023/A:1007986410048

Pang, Y., Yao, Y. H., Zhao, F., Han, F., Zhang, B., Zhang, S., & Qi, W. (2012). A method for identifying flop aspect information of mountain altitudinal belts. *Journal of Mountain Science*, *30*(3), 290–298. https://doi.org/10.1016/j.tree.2007.09.006

Perrone, M., Di Febbraro, M., Conti, L., Divíšek, J., Chytrý, M., Keil, P., Carranza, L. M., Rocchini, D., Torresani, M., Moudrý, V., Si'mová, P., Prajzlerová, D., Müllerová, J., Wild, J., & Malavasi, M. (2023). The relationship between spectral and plant diversity: Disentangling the influence of metrics and habitat types at the landscape scale. *Remote Sensing of Environment*, *293*, 113591.

Pottier, J., Malenovský, Z., Psomas, A., Homolová, L., Schaepman, M. E., Choler, P., Thuiller, W., Guisan, A., & Zimmermann, N. E. (2014). Modelling plant species distribution in alpine grasslands using airborne imaging spectroscopy. *Biology Letters*, *10*(7), 20140347. https://doi.org/10.1098/rsbl.2014.0347

Qian, D. W., Yan, C. Z., & Xiu, L. N. (2020). Land cover change and landscape pattern vulnerability response in Muli mining areas in the Qinghai-Tibet plateau. *Journal of Glaciology and Geocryology*, *42*(4), 1334–1343. https://doi.org/10.7522/j.issn.1000-0240.2018.0306

Rossi, C., Kneubühler, M., Schütz, M., Schaepman, M. E., Haller, R. M., & Risch, A. C. (2020). From local to regional: Functional diversity in differently managed alpine grasslands. *Remote Sensing of Environment*, *236*, 111415. https://doi.org/10.1016/j.rse.2019.111415

Scholtz, R., & Twidwell, D. (2022). The last continuous grasslands on earth: Identification and conservation importance. *Conservation Science and Practice*, *4*(3), 626–645. https://doi.org/10.1111/csp2.626

Shen, Z. H., Zhang, X. S., & Jin, Y. X. (2000). Gradient analysis of the influence of mountain topography on vegetation pattern. *Acta Phytoecologica Sinica*, *24*(4), 430–435. https://doi.org/10.1007/BF02876087

Tibet Autonomous Region Bureaus of Land Administration and Animal Husbandry. (1994). *Grassland resources in Tibet autonomous region*. Science Press.

Tibet Statistical Bureau. (2001-2021). *Tibet statistical yearbook Tibet statistical yearbook*. China Statistics Press.

Tibetan Plateau Comprehensive Scientific Expedition Team, & Chinese Academy of Sciences. (1983). *Tibet geomorphology*. Science Press.

Tibetan Plateau Comprehensive Scientific Expedition Team, & Chinese Academy of Sciences. (1984). *Climate in Tibet*. Science Press.

Tibetan Plateau Comprehensive Scientific Expedition Team, & Chinese Academy of Sciences. (1988). *Vegetation in Tibet*. Science Press.

Wang, C. Y., Wang, J. B., Zhang, F. W., Li, Y. N., Li, H. Q., Yang, Y. S., & Luo, F. L. (2022). Climate resource utilization rate and livestock-carrying capacity of grasslands in the three river headwaters region over the past 40 years. *Pratacultural Science*, *39*(4), 672–687. https://doi.org/10.11829/j.issn.1001-0629.2021-0601

Wang, M., Li, Y., Bai, X., & Huang, R. (2004). The impact of global warming on vegetation resources in the hinterland of the Qinghai -Tibet plateau. *Journal of Natural Resources*, *19*(3), 331–336.

Wang, X. H., & Zheng, D. (1999). Sustainable use of alpine meadow grassland resources on the Qinghai-Tibetan plateau. *Resources Science*, *21*(6), 38–42. https://doi.org/10.3321/j.issn:1007-7588.1999.06.010

Wang, Y., Sun, Y., Cao, X., Wang, Y., Zhang, W., & Cheng, X. (2023). A review of regional and global scale land use/land cover (LULC) mapping products generated from satellite remote sensing. *ISPRS Journal of Photogrammetry and Remote Sensing*, *206*, 311–334. https://doi.org/10.1016/j.isprsjprs.2023.11.014

Wang, Z. X., Liu, C., & Huete, A. (2003). From AVHRR-NDVI to MODIS-EVI: Advances in vegetation index research. Global change information and research. *Acta Ecologica Sinica*, *23*(5), 979–987. https://doi.org/10.3321/j.issn:1000-0933.2003.05.020

Weber, D., Schaepman-Strub, G., & Ecker, K. (2018). Predicting habitat quality of protected dry grasslands using Landsat NDVI phenology. *Ecological Indicators*, *91*, 447–460. https://doi.org/10.1016/j.ecolind.2018.03.081

Wen, T., Liu, X. N., Ji, T., Yang, D., Qiao, H., Jiang, J., & Pan, D. (2022). Studying on plant classification and recognition method for Three-River source alpine grassland plant based on vegetation index. *Acta Agrestia Sinica*, *30*(7), 1811–1818. https://doi.org/10.11733/j.issn.1007-0435.2022.07.023

Whittaker, R. H. (1953). A consideration of climax theory: The climax as a population and pattern. *Ecological Monographs*, *23*(1), 41–78.

Wu, J. G. (2000). *Landscape ecology: Pattern, process, scale and hierarchy*. Higher Education Press.

Xie, M. Z., Zhao, L., Wu, X. D., Zhou, H. Y., & Yue, G. Y. (2022). Seasonal variation of soil nitrogen and its relationship to environmental factors under two alpine grassland ecosystems in permafrost regions on the Qinghai-Tibet plateau. *Journal of Glaciology and Geocryology*, *44*(5), 1631–1639. https://doi.org/10.7522/j.issn.1000-0240.2022.0143

Xu, C. L. (2016). Variations in vegetation composition and nutrient characteristics related to aspect in the alpine meadow in the northeast margin of the Qinghai: Tibet plateau. *Acta Pratacultural Sinica*, *25*(4), 26–35. https://doi.org/10.11686/cyxb2015481

Yang, X. B., Zhang, W. F., Sun, B., Gao, Z., Li, Y., & Wang, H. (2022). Recognition of vegetation types in Hulunbuir Sandy land and its surrounding areas based on GEE cloud platform and Sentinel-2 time series data. *Remote Sensing Technology and Application*, *37*(4), 982–992. https://doi.org/10.11873/j.issn.1004-0323.2022.4.0982

Zhang, J., Yuan, M. S., Zhang, J., Li, H., Wang, J., Zhang, X., Ju, P., Jiang, H., Chen, H., & Zhu, Q. (2020). Responses of the NDV1 of alpine grasslands on the Qinghai-Tibetan plateau to climate change and human activities over the last 30 years. *Acta Ecologica Sinica*, *40*(18), 6269–6281. https://doi.org/10.5846/stxb201909201962

Zhang, X. S. (1978). The plateau zonality of vegetation in Xizang. *Acta Botanica Sinica*, *20*(2), 140–149.

Zhou, H., Zhou, L., Zhao, X., Liu, W., Li, Y., Gu, S., & Zhou, X. (2006). Stability of alpine meadow ecosystem on the Qinghai-Tibetan plateau. *Chinese Science Bulletin*, *51*, 320–327.

Zhu, J., Gong, J., & Li, J. Y. (2020). Spatiotemporal change of habitat quality in ecologically sensitive areas of eastern Qinghai-Tibet plateau: A case study of the Hehuang Valley, Qinghai Province. *Resources Science*, *42*(5), 991–1003. https://doi.org/10.18402/resci.2020.05.16

Zimmermann, N. E., & Kienast, F. (1999). Predictive mapping of alpine grasslands in Switzerland: Species versus community approach. *Journal of Vegetation Science*, *10*(4), 469–482.

SUPPORTING INFORMATION

Additional supporting information can be found online in the Supporting Information section at the end of this article.

How to cite this article: Chen, L., Zhang, W., Li, W., Zhang, H., Luo, S., Ran, Q., & Qin, J. (2024). Landscape changes of alpine grasslands in the Zhari Namco basin of the central-southern Qiangtang plateau, 2001–2021. *Conservation Science and Practice*, *6*(9), e13211. https://doi.org/10.1111/csp2.13211